Available online at www.sciencedirect.com
SCIENCE DIRECT®
DNA Repair 3 (2004) 1493–1502
DNA REPAIR
www.elsevier.com/locate/dnarepair

The ataxia–oculomotor apraxia 1 gene product has a role distinct from ATM and interacts with the DNA strand break repair proteins XRCC1 and XRCC4

Paula M. Clements[a], Claire Breslin[a], Emma D. Deeks[b], Philip J. Byrd[b], Limei Ju[a], Pawel Bieganowski[c], Charles Brenner[c], Maria-Céu Moreira[d], A. Malcolm R. Taylor[b], Keith W. Caldecott[a,*]

[a] *Genome Damage and Stability Centre, University of Sussex, Falmer, Brighton BN19RQ, UK*
[b] *CR-UK Institute for Cancer Studies, University of Birmingham, Edgbaston, Birmingham B152TT, UK*
[c] *Norris Cotton Cancer Center, Dartmouth Medical School, Lebanon, NH 03756, USA*
[d] *Institut de Génétique et de Biologie Moléculaire et Cellulaire, CNRS, INSERM, ULP, Strasbourg, France*

Received 19 April 2004; received in revised form 11 June 2004; accepted 14 June 2004
Available online 17 August 2004

Abstract

Ataxia–oculomotor apraxia 1 (AOA1) is an autosomal recessive neurodegenerative disease that is reminiscent of ataxia–telangiectasia (A–T). AOA1 is caused by mutations in the gene encoding aprataxin, a protein whose physiological function is currently unknown. We report here that, in contrast to A–T, AOA1 cell lines exhibit neither radioresistant DNA synthesis nor a reduced ability to phosphorylate downstream targets of ATM following DNA damage, suggesting that AOA1 lacks the cell cycle checkpoint defects that are characteristic of A–T. In addition, AOA1 primary fibroblasts exhibit only mild sensitivity to ionising radiation, hydrogen peroxide, and methyl methanesulphonate (MMS). Strikingly, however, aprataxin physically interacts in vitro and in vivo with the DNA strand break repair proteins XRCC1 and XRCC4. Aprataxin possesses a divergent forkhead associated (FHA) domain that closely resembles the FHA domain present in polynucleotide kinase, and appears to mediate the interactions with CK2-phosphorylated XRCC1 and XRCC4 through this domain. Aprataxin is therefore physically associated with both the DNA single-strand and double-strand break repair machinery, raising the possibility that AOA1 is a novel DNA damage response-defective disease.

Keywords: Ataxia–oculomotor apraxia 1; Single-strand break; Double-strand break

1. Introduction

Ataxia–oculomotor apraxia 1 (AOA1; MIM: 208920) is the most common autosomal recessive ataxia in Japan and the second most common after Friedrich's ataxia in Portugal [1,2]. AOA1 patients have a neurological presentation very similar to that of ataxia telangiectasia (ataxia–telangiectasia (A–T); MIM: 208900), in which the gene *ATM* is mutated [3]. Indeed, AOA1 was previously described as A–T-like syndrome (ATLS) [2,4]. However, the extraneurological features of A–T, such as cancer predisposition, telangiectasias, and immune deficiency, are not shared.

The gene mutated in AOA1, *APTX*, encodes a 342 amino acid protein that has been denoted aprataxin, and whose physiological function is unknown [1,2]. Aprataxin contains a Hint-like histidine triad hydrolase domain and a divergent zinc-finger motif. In addition, the amino-terminal region of aprataxin is homologous to that of polynucleotide kinase (PNK) and, as such, has been designated PNK-aprataxin amino-terminal (PANT) domain [2]. The PANT domain also harbours a forkhead-associated (FHA) motif, a phosphoprotein binding domain found in many DNA damage response proteins [5,6].

* Corresponding author. Tel.: +44 1273 877519; fax: +44 1273 678121.
E-mail address: k.w.caldecott@sussex.ac.uk (K.W. Caldecott).

1568-7864/$ – see front matter © 2004 Elsevier B.V. All rights reserved.
doi:10.1016/j.dnarep.2004.06.017

To investigate the physiological role of aprataxin, we compared DNA damage responses in AOA1 patient cells with those of A–T patient cells and wild-type controls in order to determine whether these two diseases, which share their neurological phenotype, were also similar at the cellular level. In addition, we screened a human cDNA library for binding partners of aprataxin using the yeast 2-hybrid system. Our results indicate that AOA1 is distinct from A–T at the cellular level and physically link aprataxin with the DNA ligase machinery involved in DNA single- and double-strand break repair. These data raise the possibility that a defect in the cellular response to DNA strand breaks may be involved in the neuropathology of AOA1.

2. Materials and methods

2.1. Cell culture

1BR3, 48BR and ConW are normal primary human fibroblast cell lines. AT7BI are primary A–T fibroblasts and have been described previously [7]. FD104, FD105, FD106 were provided by M.C.M. and Michel Koenig and are AOA1 primary fibroblasts, each of which is homozygous for the W279X mutation and of which FD105 and FD106 are siblings [8,9]. fAp1, fAp2 and fAp4 were provided by M.R.T. and are AOA1 primary fibroblasts harbouring the same mutation as above and of which fAp1 and fAp2 are siblings. Fibroblast cell lines were cultured in minimal essential medium supplemented with 15% foetal calf serum (FCS), L-glutamine, penicillin and streptomycin. ConR is a normal human lymphoblastoid cell line, AT156 is an A–T lymphoblastoid cell line, and Ap1 and Ap3 are AOA1 lymphoblastoid cell lines that are homozygous for the W279X mutation. Ap1 and Ap4 are from the same individuals as the primary fibroblasts, fAp1 and fAp4, respectively. Lymphoblastoid cell lines were cultured in RPMI 1640 medium with the same supplements used for fibroblast lines.

2.2. Clonogenic survival

Experiments following γ-irradiation were carried out as described previously [7]. Briefly, suitable dilutions of cells irradiated at the indicated doses were plated in triplicate onto a feeder layer. For survival experiments following MMS or H_2O_2 treatment, cells were plated onto a feeder layer (6×10^4 of the same cell type pre-irradiated with 35 Gy), and incubated overnight. MMS treatment was carried out in complete medium for 1 h at 37 °C. H_2O_2 treatment was carried out in PBS for 10 min at room temperature in the dark. All plates were incubated for 21 days and colonies of greater than 50 cells were counted following staining with methylene blue.

2.3. Measurement of RDS

Actively growing fibroblasts were labelled with 2-^{14}C-Thymidine for 3 days. Cells were then irradiated at the indicated doses and incubated with fresh medium containing [methyl-^{3}H]-Thymidine for 4 h prior to lysis (2% SDS/0.2 M NaOH). Acid precipitable ^{3}H counts were measured by liquid scintillation, normalised to ^{14}C counts, and expressed as percentage DNA synthesis relative to unirradiated cells.

2.4. Immunoblotting and immunoprecipitations

For immunoblotting human cell extracts, 2×10^6 cells were lysed in lysis buffer [20 mM Tris pH 7.5, 10 mM EDTA, 1 mM EGTA, 100 mM NaCl, 1% Triton X-100, 1 mM β-glycerophosphate, 25 mM NaF, 1 mM Na_3VO_4, and protease inhibitor cocktail (Roche Diagnostics)], and clarified extract (10–20 μg total protein) fractionated by SDS–PAGE and transferred to nitrocellulose. After incubation with primary antibodies in TBST for 1 h (see further for specific primary antibody conditions), washed immunoblots were incubated with the appropriate HRP-conjugated secondary antibody (Dako) at 1/5000 in TBST for 1 h. Washed immunoblots were then incubated with ECL detection reagents (Amersham Pharmacia Biotech). Anti-aprataxin polyclonal antibodies were raised against the amino-terminal 177 amino acids of human aprataxin and were employed at 1/2000. Anti-ATM-V and XRCC4 polyclonal antibodies were a kind gift from Steve Jackson (University of Cambridge, UK) and were employed at 1/1000. Anti-XRCC1 (AHP428) and DNA ligase IV (AHP554) polyclonal antibodies were obtained from Serotec and were employed at 1/1000 in TBST additionally containing 1% non fat dried milk (Marvel) or 5% BSA, respectively. Anti-actin monoclonal antibody was obtained from Sigma–Aldrich (Clone Ac-40) and was employed at 1/1000. Anti-Phospho-p53 and anti-Chk2 polyclonal antibodies, and Anti-Myc tag monoclonal antibodies (clone 9B11), were obtained from Cell Signalling Technologies and were employed at 1/5000 in TBST containing 5% BSA overnight (4 °C).

For co-immunoprecipitation experiments from human cell extracts, 5×10^6 wild-type or AOA1 lymphoblastoid cells were mock treated or treated with 100 μM H_2O_2 in PBS at room temperature for 10 min. Cells were then washed with PBS and incubated in fresh culture medium for 30 min before resuspension in 400 μl lysis buffer (see above). Pre-cleared cell extract (200 μg total protein) was immunoprecipitated using anti-aprataxin polyclonal antibody or irrelevant rabbit IgG (Dako) and protein G sepharose beads (Amersham Pharmacia Biotech). Fifty percent of the immunoprecipitated material together with 10% of pre-cleared input extract (20 μg total protein) was fractionated by SDS–PAGE and transferred to nitrocellulose for immunoblotting. For immunoprecipitation from yeast extracts, 250 ml cultures of Y190 cells harbouring pGBKT7-*APTX* and pACT-*XRCC1*, empty pGBTK7 and pACT-*XRCC1*, or pGBKT7-*APTX* and pACT encoding an unrelated ORF, were pelleted then resuspended in extraction buffer (100 mM KCl, 50 mM $NaPO_4$ pH8.0, 10% glycerol, 1 mM DTT, protease inhibitor

cocktail). Cells were then lysed by vortexing with acid-washed glass beads. Hundred microlitres of clarified extract (200 μg total protein) was immunoprecipitated as described above.

2.5. Immunofluorescence and chromosome aberrations

Cells were grown on coverslips for 72 h prior to treatment. For ATM and H2AX immunostaining, soluble proteins were pre-extracted from cells by incubation in ice cold pre-extraction buffer (10 mM piperazine-*NN*′-bis (2-ethanesulfonic acid), 300 mM sucrose, 3 mM $MgCl_2$, 40 mM NaCl, 0.5% Triton X-100, pH 6.8) for 5 min. Cells were then fixed in 3.6% paraformaldehyde in PBS for 10 min prior to washing (3 × 5 min in PBS), blocking in 10% FCS/PBS for 1 h, washing (3 × 5 min in PBS), and then incubation in primary anti-ATM antibody in 1% BSA/PBS for 1 h. Anti-phospho-H2AX (ser 139) mouse monoclonal antibody was obtained from Upstate Biotechnology and anti-ATM monoclonal antibody (11G12, rasied to amino acids 992–1144) has been described previously [10]. For aprataxin immunostaining, cells were fixed as above and then permeabilised in 0.5% Triton X-100/PBS for 10 min prior to blocking. Secondary antibodies were goat anti-mouse IgG1-TRITC (Southern Biotechnology Associates) for ATM immunostaining or goat anti-rabbit IgG-Alexa fluor 488 (Molecular Probes) for aprataxin immunostaining and coverslips were mounted in 0.2 μg/ml DAPI in 80% vectashield (Vector Laboratories). Immunofluorescence pictures were captured on a Nikon E600 Microscope using and ORca 100 camera and Improvision Cell Imaging system (Image Processing & Vision Company). For chromosome preparations, peripheral blood from patients was cultured for 72 h in RPMI containing 10% FCS, L-glutamine, penicillin, streptomycin and PHA. Cells were irradiated (1 Gy) and harvested after 4 h, including 1 h in colchicine. Chromosome preparations were made, stained with Giemsa and the G2 IR-induced damage analysed.

2.6. Yeast 2-hybrid analysis

Yeast Y190 cells harbouring the indicated GAL4 DNA binding [pAS or pGBKT7 (Clontech)] and activation (pACT) domain 2-hybrid constructs were plated onto minimal media lacking Leu and Trp to select for both plasmids or on media additionally lacking histidine and containing 25 mM 3-aminotriazole to select for histidine prototrophy, which is indicative of a protein–protein interaction. In addition, colonies from Leu-, Trp- control plates were examined for β-galactosidase activity by filter lift assays as a second test for protein–protein interaction. For liquid β-galactosidase assays, minimal media cultures (50 ml, supplemented with adenine and histidine) were cultured to an $O.D._{600}$ of 0.5–0.8 from 5 ml starter cultures of single Y190 clones (inoculated from fresh YEPD plates streaked from a glycerol stock) harbouring the appropriate pAS/pGBKT7 and pACT constructs. Cells were recovered from 40 ml of each culture by centrifugation and lysed in 0.3–0.4 ml of Cracking Buffer (8 M urea, 5% SDS, 40 mM Tris–Cl pH 6.8, 0.1 M EDTA pH 8, 0.4 mg/ml bromophenol blue). Five microlitres aliquots were fractionated by SDS–PAGE and transferred to nitrocellulose for immunoblotting with anti-aprataxin antibodies or with anti-GAL4 AD polyclonal antibodies (Upstate Biotechnology). Cells from the remaining 10 ml of each culture were pelleted and used to measure β-galactosidase activity as directed in the Clontech Yeast Protocols Handbook, using red-β-D-galactopyranoside (CPRG) as a substrate.

2.7. Recombinant proteins and dot/slot blotting

Human aprataxin cDNA was inserted into the bacterial His-tag expression vector pSGA04 [11] by P.B. and C.B. to generate plasmid pB352. pET16b (Novagen) containing the human XRCC1 [pET16bXH; [12]] and XRCC4 (pET16b-HisXRCC4; this study) ORFs was employed for expression of these human proteins expressed in BL21(DE3) as C-terminal and amino-terminal histidine-tagged ORFs, respectively. Recombinant ^{35}S-labelled or unlabelled proteins were purified by metal chelate chromatography and, in the case of ^{35}S-labelled XRCC1, anion exchange chromatography. ^{35}S-labelled XRCC1 and XRCC4 were prepared essentially as described [13]. Briefly, IPTG was added to 1 mM to 50 ml BL21(DE3) cultures ($O.D._{600}$ of 0.6) in M9 media for 30 min at 30 °C, followed by addition of rifampicin (from a 10 mg/ml stock in methanol) to 0.2 mg/ml for a further 30 min to inhibit bacterial RNA polymerase, followed by addition of 20 μl (200 μCi) of ^{35}S-methionine (Amersham; >1000 Ci/mmol) for a further 2–3 h at 30 °C. 0.5 μg (slot blots) or 3 μg (dot blots) of recombinant human full length aprataxin, an amino terminal fragment of aprataxin containing the FHA domain ($aprataxin^{1-152}$), or BSA negative control was dot-blotted (for ^{35}S-XRCC1 probes) or, in later experiments, slot blotted (for ^{35}S-XRCC4 probes) onto nitrocellulose and the filters blocked for 30 min at 4 °C in binding buffer containing 1% non-fat dried milk. Filters were then incubated at 4 °C in binding buffer containing 1 μg/ml ^{35}S-XRCC1 and 1% non-fat dried milk overnight, or 50 μg/ml ^{35}S-XRCC4 without non-fat dried milk for 3 h. Filters were rinsed briefly in binding buffer, dried, and analysed by phosphorimager. Binding buffer for experiments employing ^{35}S-XRCC1 was 20 mM Hepes pH 8, 100 mM KCl, 2.5 mM $MgCl_2$, 0.05% Tween 20, and 1 mM DTT, and for ^{35}S-XRCC4 was 25 mM Tris–Cl, pH 7.5, 100 mM NaCl, 1 mM DTT. ^{35}S-XRCC1 or ^{35}S-XRCC4 probes were mock-phoshorylated or phosphorylated in the presence of 10 mM $MgCl_2$ and 1 mM ATP in either ^{35}S-XRCC4 binding buffer (for ^{35}S-XRCC4) or 20 mM Tris–Cl pH 7.0, 130 mM KCl, 5 mM DTT, 5% glycerol (for ^{35}S-XRCC1) containing either recombinant human CK2 (Roche; 1 mU in 230 μl total volume) for experiments employing ^{35}S-XRCC1 or, in later experiments employing ^{35}S-XRCC4, rat liver CK2 provided by Flavio Meggio and Lorenzo A. Pinna.

3. Results

To investigate the molecular basis of AOA1, we have utilised a number of lymphoblastoid cell lines and primary fibroblasts from individuals with this disease. Sequencing of amplified *APTX* cDNA revealed that each of these individuals were homozygous for the nonsense mutation W279X [[8,9] and A.M.R. Taylor unpublished results], previously identified as the founding haplotype in the Portuguese population [2]. Immunoblotting with anti-aprataxin antibodies, raised against the amino-terminal 177 amino acids of the polypeptide, demonstrated that full-length aprataxin (~36 kDa) was absent from AOA1 individuals (Fig. 1a). We also failed to detect a truncated fragment of aprataxin of the size expected, based on the position of the nonsense mutation (data not shown). This suggests that the W279X mutation results in decreased stability of the *APTX* mRNA or the truncated polypeptide. Given the similarity in neurological phenotype of AOA1 with A–T, we also examined the level of ATM and aprataxin in AOA1 and A–T primary fibroblasts. ATM levels were absent from an A–T cell line but were similar to that observed in wild-type cells in three separate AOA1 cell lines (Fig. 1a). Similarly, the level of aprataxin in the A–T cell line was comparable to that observed in wild-type cells. The levels of XRCC1 and XRCC4, proteins involved in DNA single-strand and double-strand break repair, respectively, were normal in both A–T and AOA1 cells. Immunofluorescence experiments were then conducted to examine the sub-cellular distribution of aprataxin (Fig. 1b). Diffuse staining of aprataxin was visible in the nuclei of normal fibroblasts but was absent from AOA1 fibroblasts, indicating that aprataxin is primarily a nuclear protein.

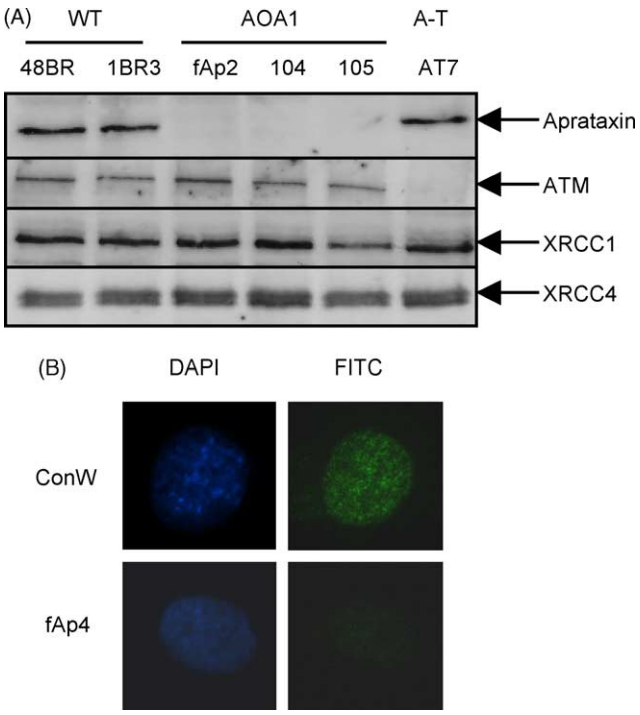

Fig. 1. Aprataxin protein in wild type and AOA1 primary human fibroblasts. (A) Cell extracts from wild-type (48BR, 1BR3), AOA1 (fAp2, 104, 105), and A–T (AT7BI) primary human fibroblasts were immunoblotted for aprataxin, XRCC1, XRCC4, and ATM proteins. (B) Sub-cellular distribution of aprataxin in normal (ConW) and AOA1 (fAp4) primary human fibroblasts as measured by indirect immunofluorescence using anti-aprataxin antibodies (FITC) and counterstaining with DAPI.

A characteristic feature of A–T cells is radio-resistant DNA synthesis (RDS), a phenotype indicative of a defect in the intra S-phase cell cycle checkpoint [14]. We therefore examined whether AOA1 cells also displayed RDS. Primary fibroblasts from three separate AOA1 patients were each able to suppress DNA synthesis following γ-rays to a level comparable to that observed in two wild-type primary fibroblast cell lines (Fig. 2a). This was in contrast to primary A–T fibroblasts, which displayed the RDS phenotype previously reported for this disease.

A second hallmark of the cell cycle checkpoint defect in A–T cells is reduced or delayed phosphorylation of p53 and Chk2 following DNA damage [15–17]. We therefore compared wild-type lymphoblastoid cells with those from AOA1 and A–T patients for levels of phosphorylated p53 (serine-15) and Chk2 (threonine 68). AOA1 and wild-type lymphoblastoid cells accumulated similar levels of phosphorylated p53 and Chk2 during a 7h time course following γ-radiation (Fig. 2b). The same was observed following exposure to 100 μM H_2O_2 (data not shown). This was in contrast to A–T lymphoblastoid cells, which displayed the expected reduced or delayed ability to accumulate phosphorylated Chk2 and p53 over this time period. In the experiment shown above, AOA1 cells appeared to attenuate their Chk2 response before wild type cells (Fig. 2b, 7 h time point). However, this did not appear to be a consistent feature of AOA1 cells.

AOA1 primary fibroblasts were also examined for their ability to form phosphorylated H2AX (γ-H2AX) and ATM foci, both of which are formed at sites of DNA double-strand breaks in wild type cells [18,19]. Formation of ATM foci and their co-localisation with γ-H2AX was normal in AOA1 fibroblasts at 7 h following treatment with H_2O_2 (Fig. 2c) suggesting that aprataxin is not required for relocation of ATM to sites of double-strand breaks. Interestingly, we failed to observe the appearance of aprataxin foci in wild type cells under the same conditions (data not shown) suggesting that aprataxin differs from ATM in its sub-cellular distribution after DNA damage.

Another hallmark feature of A–T cells that is also believed to result from a cell cycle checkpoint or DNA repair defect, is increased levels of chromosomal aberrations. However, AOA1 cells were distinct from A–T cells in this respect also, with levels of chromosomal aberrations following irradiation in G2 similar in AOA1 lymphocytes to those observed in wild type lymphocytes (Table 1). Irradiation in G_0 gave similar results, with AOA1 lymphocytes lacking the high frequency of chromatid damage, including triradials and quadriradials, associated with irradiated A–T lymphocytes (data not shown).

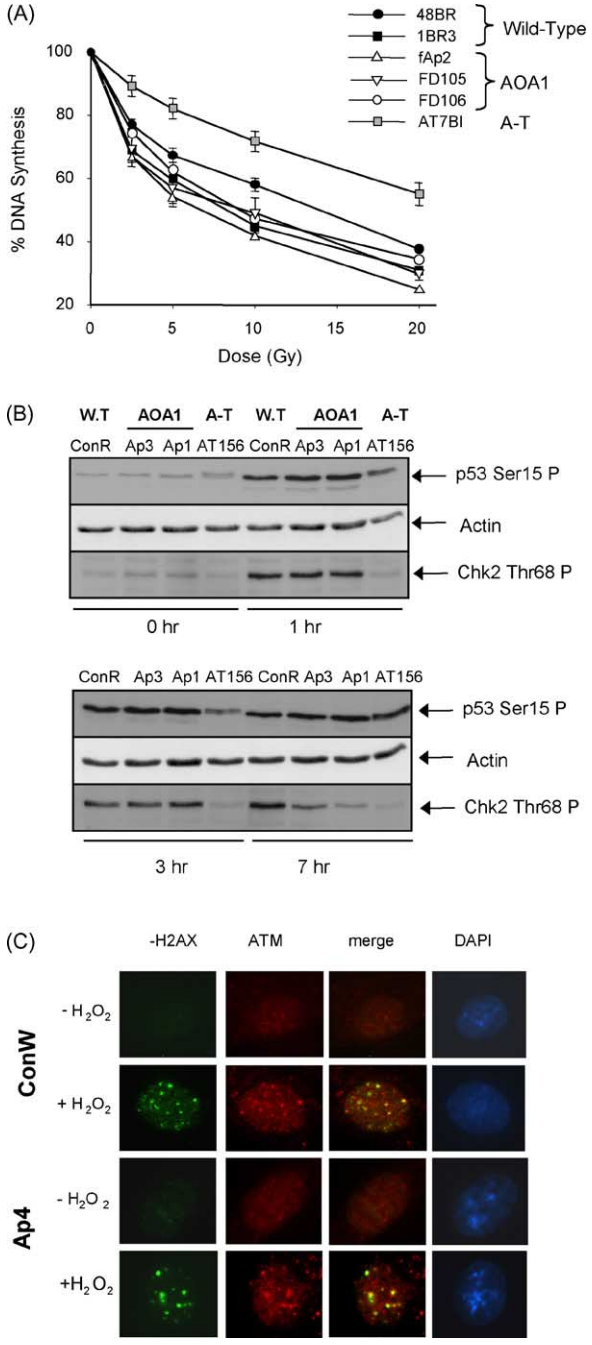

Fig. 2. Investigation of ATM-dependent DNA damage responses in AOA1 cells. (A) Radio-resistant synthesis in A–T but not AOA1 cells. The indicated wild-type (48BR, 1BR3), AOA1 (fAp2, FD105, FD106), and A–T (AT7BI) primary fibroblasts were treated with γ-rays at the doses indicated and the level of DNA synthesis occurring during the following 4 h was quantified, relative to untreated cells. Data represent the mean ± S.E.M. of three independent experiments. Where not shown, error bars are smaller than symbols. (B) The indicated wild-type (ConR), AOA1 (Ap1, Ap3), and A–T (AT156) lymphoblastoid cell lines were harvested at the indicated time points after γ-irradiation (2 Gy) or mock-irradiation and immunoblotted with anti-phospho p53 (Ser15), anti-phospho Chk2 (Thr68), or anti-actin antibodies. (C) Co-localisation of γ-H2AX and ATM in wild-type (ConW) and AOA1 (fAp4) primary human fibroblasts 7 h after treatment, or mock-treatment, with H_2O_2 (10 mM). Immunostaining was conducted on cells that were fixed following pre-extraction with detergent, and cells were counterstained with DAPI.

Table 1
X-ray (1.0 Gy) induced chromosome damage in lymphocytes from AOA1 patients Ap3, Ap4, and A–T cells following exposure to X-rays in G2

Individual	Cells	Frag	tg	tb	cg	cb	Interch
Ap 3	50	0	4	1	0	0	0
Ap 4	50	0	3	1	0	0	0
Normal	50	0	8	0	0	0	0
Classical A–T	50	2	40	10	0	0	6

frag: Fragments; tg: chromatid gaps; tb: chromatid breaks; cg: chromosome gaps; cb: chromosome breaks; Interch.: chromatid interchanges (triradials and quadriradials).

Finally, a fourth hallmark feature of A–T is cellular hypersensitivity to ionising radiation [20]. We therefore compared four AOA1 primary fibroblast cell lines with wild-type controls and A–T cells for clonogenic survival following γ-rays. As was observed for the intra-S phase checkpoint, AOA1 cells and A–T cells were clearly distinct in their response to γ-rays, with A–T cells exhibiting much greater sensitivity than AOA1 fibroblasts (Fig. 3a). However, only a mild increase in sensitivity to γ-rays was observed in AOA1 cells, though this sensitivity was statistically significant (P-values ranging from 0.009 to 0.031) at all doses except 5 Gy (due to the large error bars for this data point). Mild sensitivity of AOA1 primary fibroblasts was also observed with the alkylating agent MMS (Fig. 3b) and the oxidising agent, H_2O_2 (Fig. 3c).

The results described above strongly suggest that AOA1 does not share the cell cycle checkpoint defects that are characteristic of A–T. To further investigate the molecular role of aprataxin we screened a human cDNA library for interacting partners using the yeast 2-hybrid assay. For this purpose, full-length human *APTX* was subcloned into pGBKT7, a GAL4 DNA binding domain vector. A total of 2.3×10^6 independent transformants were screened for histidine prototrophy. Four independent clones were recovered which encoded the C-terminal region of XRCC1, a scaffold protein that plays a critical role in the repair of chromosomal DNA single-strand breaks [21]. An additional four independent clones were recovered encoding all but the amino-terminal region of XRCC4, a protein which plays a critical role in the repair of chromosomal DNA double-strand breaks by non-homologous end joining (NHEJ) [22]. Both of these proteins are physically bound in mammalian cells with DNA ligases; DNA Ligase IIIα in the case of XRCC1, and DNA Ligase IV in the case of XRCC4 [13,23,24]. To confirm the specificity of these interactions, pACT constructs encoding full length *XRCC1* or *XRCC4* were introduced into yeast Y190 cells together with pGBKT7-*APTX* or with appropriate negative controls (Fig. 4). Whereas yeast Y190 cells harbouring pGBKT7-*APTX* and either pACT-*XRCC1* or pACT-*XRCC4* activated both the histidine and β-galactosidase reporter genes, Y190 cells harbouring each of these plasmids with a variety of negative controls did not. That full-length XRCC1 was able to interact with aprataxin in vivo was also confirmed by a reciprocal yeast 2-hybrid screen employing XRCC1 as

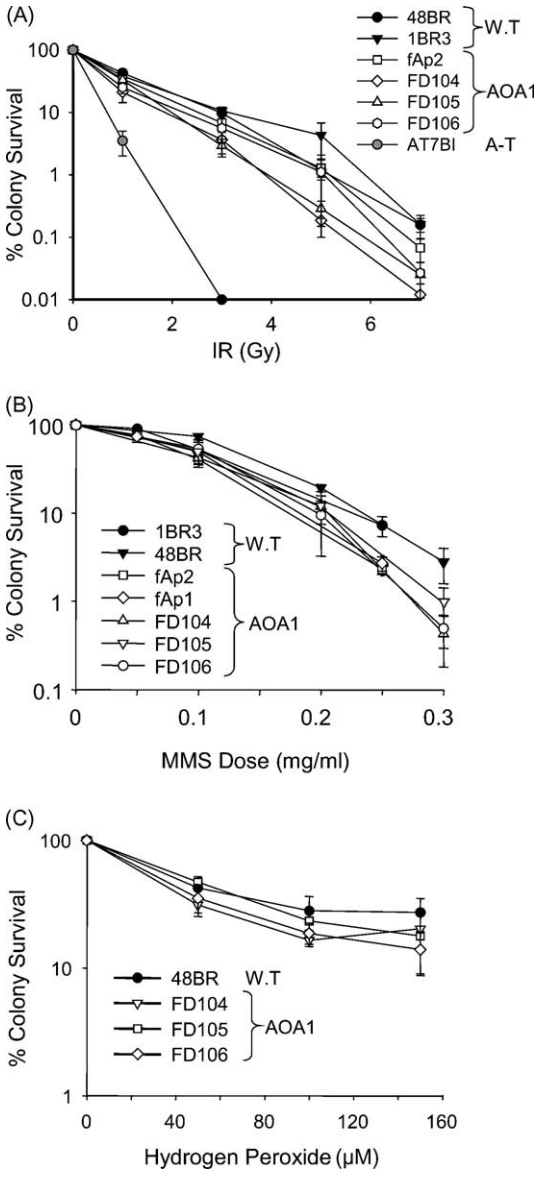

Fig. 3. Clonogenic survival of AOA1 primary human fibroblasts following exposure to genotoxins. Wild-type (48BR, 1BR3), AOA1 (fAp1, fAp2, FD104, FD105, FD106), and A–T (AT7BI) primary fibroblasts were treated with γ-irradiation (A), MMS (B), or H_2O_2 (C) at the indicated doses and the surviving fraction was quantified by dividing the number of macroscopic colonies present after 21 days on treated plates by the number on untreated plates. Data are the mean (±S.E.M.) of at least three independent experiments.

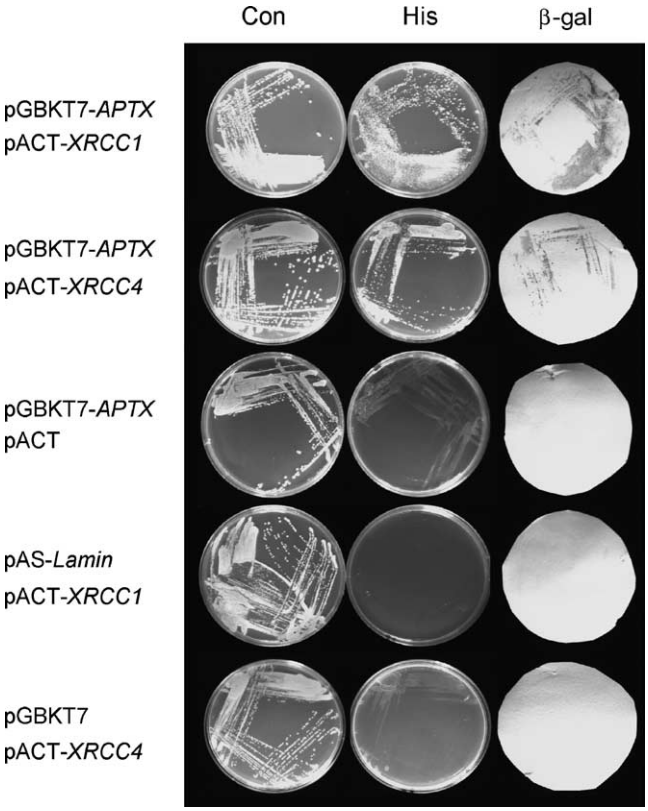

Fig. 4. Aprataxin interacts with XRCC1 and XRCC4 in vivo. Yeast Y190 cells harbouring the indicated constructs were plated onto minimal media control plates lacking leucine and tryptophan to maintain selection for the indicated constructs ("Con"), or onto minimal media plates additionally lacking histidine and containing 25 mM 3-aminotriazole ("His") to select for protein–protein interaction. The presence or absence of protein–protein interaction was also assessed by β-galactosidase ("βgal") assays on cells filter-lifted from a minimal media control plate lacking leucine and tryptophan.

bait, in which two independent *APTX* cDNA clones were recovered (data not shown).

The interaction between aprataxin and XRCC1 or XRCC4 was also observed in vitro, in co-immunoprecipitation experiments. Aprataxin was immunoprecipitated from extracts from either Y190 cells harbouring pGBKT7-*APTX* and pACT-*XRCC1* by anti-XRCC1 antibodies (Fig. 5a, lane 2), or Y190 cells harbouring pGBKT7-*APTX* and pACT-XRCC4 by anti-XRCC4 antibodies (Fig. 5a, lane 4). This was not the case in control immunoprecipitations employing extracts from Y190 cells harbouring empty pGBTK7 and either pACT-*XRCC1* (Fig. 5a, lane 1) or pACT-XRCC4 (Fig. 5a, lane 5). More importantly, aprataxin was not immunoprecipitated by anti-XRCC1 or anti-XRCC4 antibodies from extracts from Y190 cells harbouring pGBTK7-*APTX* and an unrelated pACT construct (Fig. 5a, lanes 3 and 6). This confirms that aprataxin was only precipitated by anti-XRCC1 or anti-XRCC4 antibody if XRCC1 or XRCC4 were present.

XRCC1 and its binding partner DNA Ligase IIIα were also co-immunoprecipitated by anti-aprataxin polyclonal antibodies from cell extracts prepared from untreated human cells or from human cells pre-treated with H_2O_2 (Fig. 5b). In contrast, rabbit IgG failed to recover XRCC1 in control immunoprecipitations conducted in parallel. More importantly, XRCC1 was not recovered by anti-aprataxin antibody from AOA1 cell extracts lacking aprataxin. Immunoblotting with anti-aprataxin antibody confirmed that, where present, aprataxin was immunoprecipitated successfully in these experiments (Fig. 5b). The presence of XRCC4 in aprataxin immunocomplexes could not be determined directly because XRCC4 could not be separated from the IgG heavy chain

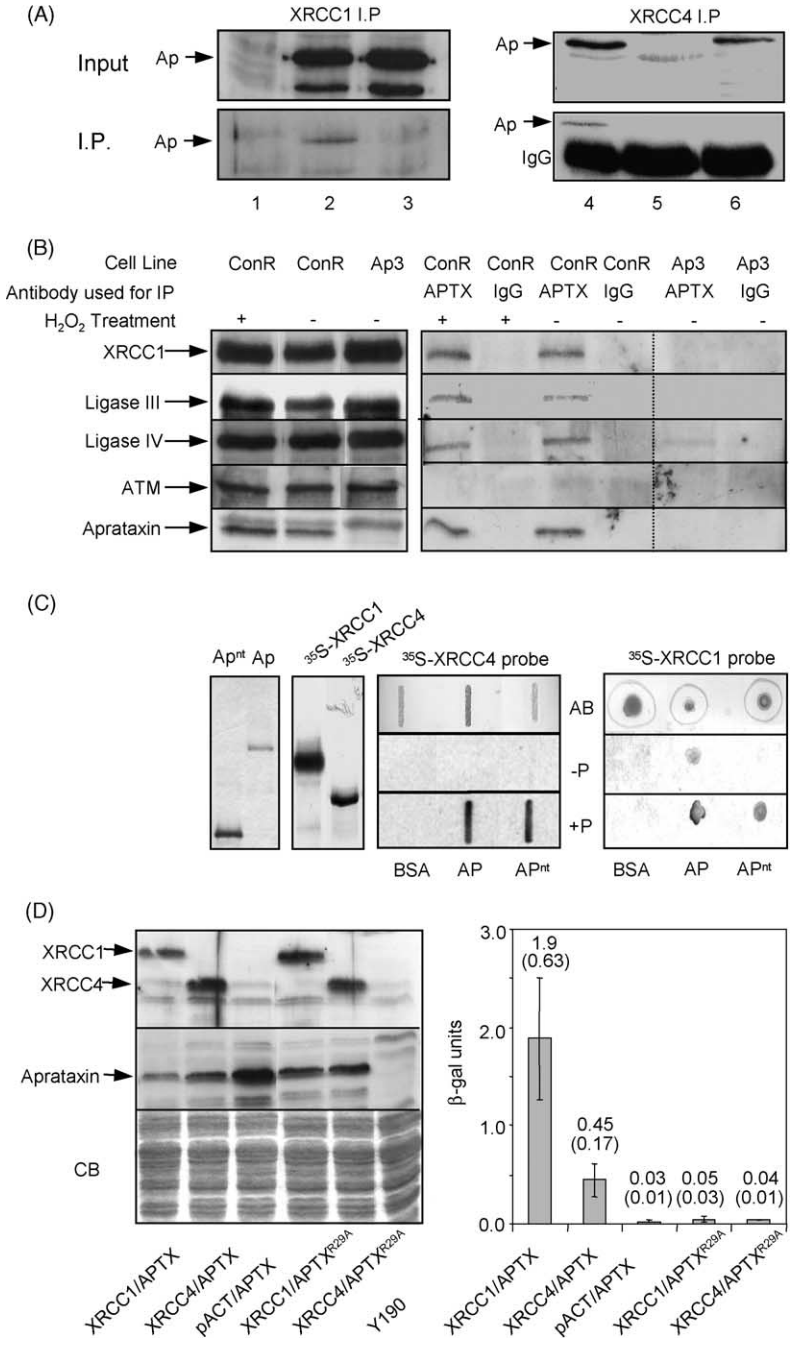

Fig. 5. The FHA domain of aprataxin interacts with XRCC1 and XRCC4. (A) XRCC1 was immunoprecipitated from protein extract (200 μg total protein) from yeast Y190 cells harbouring empty pGBKT7 and pACT-*XRCC1* (lane 1), pGBKT7-*APTX* and pACT-*XRCC1* (lane 2), or pGBKT7-*APTX* and pACT containing an unrelated ORF (lane 3). XRCC4 was immunoprecipitated from protein extract (200 μg total protein) from yeast Y190 cells harbouring pGBKT7-*APTX* and pACT-*XRCC4* (lane 4), empty pGBKT7 and pACT-*XRCC4* (lane 5), or pGBKT7-*APTX* and pACT containing an unrelated ORF (lane 6). Cell extract prior to immunoprecipitation ("Input"; 20 μg total protein) and the immunoprecipitated material ("I.P") was immunoblotted with anti-aprataxin antibody to locate aprataxin ("Ap"). (B) Protein extract from untreated or H_2O_2-treated (100 μM) wild-type (ConR) or AOA1 (Ap3) lymphoblastoid cells was immunoprecipitated with anti-aprataxin ("APTX") or control rabbit IgG ("IgG") and aliquots of input extract (left panels, 20 μg total protein) and immunoprecipitates (right panel) were immunoblotted with anti-XRCC1, anti-DNA Ligase IIIα, anti-DNA Ligase IV, anti-ATM, or anti-aprataxin antibodies. (C) Full length aprataxin (Ap), aprataxin$^{1-152}$ (Ap^{nt}), and BSA were dot blotted onto nitrocellulose in triplicate and filters either stained with amido black ("AB") or incubated with mock-phosphorylated ("–P") or CK2-phosphorylated ("+P") ^{35}S-XRCC1 or ^{35}S-XRCC4 probe, as indicated. Aliquots of the aprataxin polypeptides (first panel from left), and the two probes prior to phosphorylation or mock-phosphorylation (second panel from left), were fractionated by SDS–PAGE and detected with coomassie blue or autoradiography, respectively, to confirm purity. (D) Aliquots of logarithmic cultures Y190 cells harbouring pGBTK7-APTX or pGBTK7-APTX^{R29A} and either empty pACT, pACT-XRCC1, or pACT-XRCC4, were (left panel) fractionated by SDS–PAGE, transferred to nitrocellulose, and immunoblotted with anti-aprataxin polyclonal antibodies or with anti-GAL4 AD antibodies (to detect XRCC1 or XRCC4) or were (right panel) employed for liquid β-galactosidase assays to quantitate levels of protein–protein interaction. Values above bars are the mean of three independent experiments (±1S.E.).

by SDS–PAGE (data not shown). However, the constitutive binding partner of XRCC4, DNA Ligase IV, was co-immunoprecipitated by anti-aprataxin antibodies but not rabbit IgG control antibodies, from extracts prepared from untreated or H_2O_2-treated cells (Fig. 5b). More importantly, as observed with XRCC1, anti-aprataxin antibody failed to recover DNA ligase IV from AOA1 cell extracts lacking aprataxin. It was noteworthy that the level of XRCC1 and DNA Ligase IV co-immunoprecipitated by anti-aprataxin antibody from wild type cells was not significantly altered by pre-treatment with H_2O_2, suggesting that the interaction of aprataxin with XRCC1 and XRCC4 is largely constitutive. It was also noted that neither rabbit IgG nor anti-aprataxin antibodies recovered ATM from human cell extracts, suggesting that aprataxin and ATM are not measurably co-associated before or after DNA damage (Fig. 5b).

The presence of an FHA domain at the amino-terminus of aprataxin [5] suggests that the interaction of this polypeptide with XRCC1 and/or XRCC4 may be regulated by phosphorylation. Indeed, the FHA domain of aprataxin is highly homologous to the FHA domain present at the amino-terminus of PNK, which interacts with a cluster of CK2 phosphorylation sites in XRCC1 [5,25]. Examination of the protein sequence of XRCC4 also revealed the presence of several putative CK2 phosphorylation sites in this protein, and it was noticed that these sites were present in all of the truncated XRCC4 clones recovered in the yeast 2-hybrid screen. We therefore examined directly whether interaction of XRCC1 and XRCC4 with aprataxin may be dependent on phosphorylation by CK2 in vitro. Histidine-tagged full-length aprataxin and an amino-terminal fragment containing the FHA domain were expressed in *Escherichia coli*, purified by metal chelate chromatography and dot-blotted onto nitrocellulose along with BSA. The filters were then incubated with mock-phosphorylated or CK2 phosphorylated ^{35}S-XRCC1 or ^{35}S-XRCC4 probes (Fig. 5c). Approximately eight-fold more CK2-phosphorylated ^{35}S-XRCC1 was bound by the amino-terminal fragment of aprataxin than was mock-phosphorylated ^{35}S-XRCC1. A comparable level of phosphorylated ^{35}S-XRCC1 probe was bound by full-length aprataxin, and this binding was reduced approximately three-fold if mock-phosphorylated XRCC1 was employed as a probe. Similar results were observed for XRCC4. Whereas CK2-phosphorylated ^{35}S-XRCC4 readily bound both the amino-terminal fragment and full-length aprataxin, mock-phosphorylated ^{35}S-XRCC4 did not. Both ^{35}S-XRCC1 and ^{35}S-XRCC4 probes failed to bind BSA negative control in these experiments, irrespective of whether or not the probes were first phosphorylated with CK2. A critical role for phosphorylation for interaction between XRCC1, XRCC4, and aprataxin was further supported by yeast 2-hybrid experiments, since mutation of a critical arginine residue (R29A) within the aprataxin FHA domain reduced the interaction of aprataxin with XRCC1 and XRCC4 by more than ten-fold, to background levels, as measured by quantitative liquid β-galactosidase assays (Fig. 5D). Arg29 corresponds to the structurally and functionally essential Arg70/Arg117 in the Rad53/Chk2 FHA domains, respectively [6], and we have shown previously that the analogous mutation in the FHA domain of PNK (R35A) greatly reduces or ablates interaction with XRCC1 [25]. Together, these data suggest that aprataxin binds XRCC1 and XRCC4 in a phosphorylation-dependent manner, most likely via an FHA domain present in the amino-terminus of aprataxin.

4. Discussion

Individuals with AOA1 have a neurological presentation that is very similar to that of ataxia telangiectasia (A–T; MIM: 208,900), in which the gene *ATM* is mutated [3]. Indeed, AOA1 was previously described as A–T-like syndrome (ATLS) [2,4]. However, the extraneurological features of A–T, such as telangiectasias, immune deficiency, and cancer predisposition, are not shared. Whereas the molecular role of ATM has been intensively examined, the role of aprataxin, the gene product mutated in AOA1, is unknown. In this study we have begun to address this issue by comparing the cellular phenotypes of A–T and AOA1 primary fibroblasts and lymphoblastoid cell lines. In addition, we have identified novel interactions between aprataxin and the polypeptides XRCC1 and XRCC4, components of the DNA single-strand break repair and DNA double-strand break repair machinery, respectively.

A comparison of AOA1 and A–T cell lines revealed that AOA1 does not possess the chromosome instability or cell cycle checkpoint defects characteristic of A–T, and it is tempting to speculate that this difference accounts for the apparent lack of cancer predisposition in AOA1. Conversely, the similarity in neurological phenotype of AOA1 and A–T suggests that the neurodegeneration in A–T may not be caused by defects in cell cycle checkpoints. Neurodegeneration in A–T could result from an inability to trigger apoptosis in response to unrepaired double strand breaks [26]. This is suggested by the observed role for ATM in triggering apoptosis in the developing nervous system of mice exposed to ionising radiation or lacking the non homologous end joining protein, DNA ligase IV [27]. In the absence of ATM, cells with unrepaired DNA double-strand breaks may persist and ultimately result in neuronal dysfunction and degeneration. In addition, ATM may also play a role in the repair of DNA double-strand breaks, resulting in even greater numbers of damaged cells in the nervous system in A–T. Mice lacking DNA polymerase β also exhibit high levels of apoptosis in the developing nervous system suggesting that unrepaired DNA single-strand breaks are also a threat to the nervous system [28]. Given the interaction of aprataxin with XRCC1 and XRCC4, neurodegeneration in AOA1 could thus similarly result from an inability to either repair DNA single- or double-strand breaks or to signal the presence of unrepaired breaks to the apoptotic machinery. We have so far failed to detect a measurable defect in DNA strand-break repair processes in AOA1, at least

in lymphoblastoid cells and cycling or quiescent primary fibroblasts (P.M.C unpublished observations). The interaction between XRCC1 and aprataxin has also been reported by two other groups, one of which similarly did not find a gross defect in single-strand break repair in AOA1 cells [29,30]. The minor sensitivity of AOA1 cells to alkylating agents and γ-rays, and the lack of apparent chromosome instability, also argues against a major requirement for aprataxin for DNA single- or double-strand break repair, although a subtle role or a requirement specifically in neurons has not been ruled out. It should be noted, however, that Gueven et al. reported a more marked sensitivity to H_20_2 and MMS in AOA1 lymphoblastoid cell lines than that reported here for AOA1 primary fibroblasts, and also an absence of sensitivity to IR [29]. This discrepancy my reflect the different cell types, cytotoxicity assays, or AOA1 mutations employed in the two studies.

The interaction between aprataxin and both XRCC1 and XRCC4 required phosphorylation of the latter two proteins by CK2, and mutation of a critical arginine residue within the aprataxin FHA domain greatly reduced or ablated ablated interaction with XRCC1 and XRCC4. We have recently demonstrated that CK2 facilitates chromosomal single-strand break repair in part by stimulating binding of the polynucleotide kinase (PNK) FHA domain to a cluster of CK2 sites in XRCC1 [25]. The FHA domains in aprataxin and PNK are very similar, much more so to each other than to other FHA domains, suggesting that aprataxin may bind these same sites in XRCC1 [5]. Indeed, mutation of eight primary CK2 sites within the cluster in XRCC1 greatly reduces or ablates the interaction with both PNK [25] and aprataxin (K.W.C., unpublished observations). It is not yet clear whether aprataxin and PNK both bind XRCC1 together, compete for binding to XRCC1, bind XRCC1 consecutively, or whether they are present in distinct and separate XRCC1 complexes. Intriguingly, a similar situation may exist with XRCC4. PNK is involved in NHEJ [31], and we have observed that an amino terminal fragment of PNK encoding the FHA domain interacts with CK2-phosphorylated XRCC4 (Joanna Loizou and K.W.C, unpublished observations). It remains to be determined, however, whether aprataxin and PNK bind the same CK2 sites in XRCC4.

The biochemical role of aprataxin is unclear. This protein appears to be a member of the Hint subfamily of HIT proteins, exhibiting 30% identity with the active site of rabbit and human Hint1. Rabbit hint1 exhibits adenosine monophosphoramidase activity, during which AMP is released from substrate molecules that can be defined as AMP-X, where X is a small molecule or possibly a polypeptide [32]. Based on this, it was suggested that Hint proteins may de-adenylate polypeptides, thereby modifying their activity. Aprataxin may thus modify the activity of XRCC1 or XRCC4, or perhaps regulate the adenylation status of DNA ligase IIIα or DNA ligase IV. Future experiments will hopefully identify the critical substrates of aprataxin, and also shed light on the hypotheses that this important polypeptide either influences single- or double-strand break repair in some way or interfaces with the signal transduction machinery.

In summary, we have demonstrated that primary fibroblasts and lymphoblastoid cell lines from individuals with the ataxia telangiectasia-like disorder ataxia–oculomotor apraxia 1 lack the high levels of radiosensitivity, chromosome instability, and cell cycle checkpoint defects characteristic of A–T. This suggests that the role of the AOA1 gene product aprataxin is distinct from that of ATM and provides a possible explanation for the absence of cancer in AOA1. In addition, we report that aprataxin interacts in vivo and in vitro with the DNA single- and double-strand break repair proteins XRCC1 and XRCC4, apparently via an FHA domain in aprataxin and CK2 phosphorylation sites in XRCC1 and XRCC4. These data raise the possibility that AOA1 is a novel type of DNA damage response-defective disease.

References

[1] H. Date, O. Onodera, H. Tanaka, K. Iwabuchi, K. Uekawa, S. Igarashi, R. Koike, T. Hiroi, T. Yuasa, Y. Awaya, T. Sakai, T. Takahashi, H. Nagatomo, Y. Sekijima, I. Kawachi, Y. Takiyama, M. Nishizawa, N. Fukuhara, K. Saito, S. Sugano, S. Tsuji, Early-onset ataxia with ocular motor apraxia and hypoalbuminemia is caused by mutations in a new HIT superfamily gene, Nat. Genet. 29 (2001) 184–188.

[2] M.C. Moreira, C. Barbot, N. Tachi, N. Kozuka, E. Uchida, T. Gibson, P. Mendonca, M. Costa, J. Barros, T. Yanagisawa, M. Watanabe, Y. Ikeda, M. Aoki, T. Nagata, P. Coutinho, J. Sequeiros, M. Koenig, The gene mutated in ataxia-ocular apraxia 1 encodes the new HIT/Zn-finger protein aprataxin, Nat. Genet. 29 (2001) 189–193.

[3] K. Savitsky, A. Bar-Shira, S. Gilad, G. Rotman, Y. Ziv, L. Vanagaite, D.A. Tagle, S. Smith, T. Uziel, S. Sfez, A single ataxia telangiectasia gene with a product similar to PI-3 kinase, Science 268 (1995) 1749–1753.

[4] A.H. Nemeth, E. Bochukova, E. Dunne, S.M. Huson, J. Elston, M.A. Hannan, M. Jackson, C.J. Chapman, A.M. Taylor, Autosomal recessive cerebellar ataxia with oculomotor apraxia (Ataxia–Telangiectasia-like syndrome) is linked to chromosome 9q34, Am. J. Hum. Genet. 67 (2000) 1320–1326.

[5] K.W. Caldecott, DNA single-strand break repair and spinocerebellar ataxia, Cell 112 (2003) 7–10.

[6] D. Durocher, S.P. Jackson, The FHA domain, FEBS Lett. 513 (2002) 58–66.

[7] C.F. Arlett, S.A. Harcourt, Survey of radiosensitivity in a variety of human cell strains, Cancer Res. 40 (1980) 926–932.

[8] B. Le, I.M.C. Moreira, S. Rivaud-Pechoux, C. Chamayou, F. Ochsner, T. Kuntzer, M. Tardieu, G. Said, M.O. Habert, G. Demarquay, C. Tannier, J.M. Beis, A. Brice, M. Koenig, A. Durr, Cerebellar ataxia with oculomotor apraxia type 1: clinical and genetic studies, Brain 126 (2003) 2761–2772.

[9] C. Tranchant, M. Fleury, M.C. Moreira, M. Koenig, J.M. Warter, Phenotypic variability of aprataxin gene mutations, Neurology 60 (2003) 868–870.

[10] J. Starczynski, W. Simmons, J.R. Flavell, P.J. Byrd, G.S. Stewart, H.S. Kullar, A. Groom, J. Crocker, P.A. Moss, G.M. Reynolds, M. Glavina-Durdov, A.M. Taylor, C. Fegan, T. Stankovic, P.G. Murray, Variations in ATM protein expression during normal lymphoid differentiation and among B-cell-derived neoplasias, Am. J. Pathol. 163 (2003) 423–432.

[11] S. Ghosh, J.M. Lowenstein, A multifunctional vector system for heterologous expression of proteins in *Escherichia coli*. Expression of native and hexahistidyl fusion proteins, rapid purification of the fusion proteins, and removal of fusion peptide by Kex2 protease, Gene 176 (1996) 249–255.
[12] K.W. Caldecott, J.D. Tucker, L.H. Stanker, L.H. Thompson, Characterization of the XRCC1-DNA ligase III complex in vitro and its absence from mutant hamster cells, Nucleic Acids Res. 23 (1995) 4836–4843.
[13] K.W. Caldecott, C.K. Mckeown, J.D. Tucker, S. Ljungquist, L.H. Thompson, An interaction between the mammalian DNA repair protein XRCC1 and DNA ligase III, Mol. Cell Biol. 14 (1994) 68–76.
[14] R.B. Painter, B.R. Young, Radiosensitivity in Ataxia–Telangiectasia: a new explanation, Proc. Natl. Acad. Sci. U.S.A 77 (1980) 7315–7317.
[15] S. Banin, L. Moyal, S. Shieh, Y. Taya, C.W. Anderson, L. Chessa, N.I. Smorodinsky, C. Prives, Y. Reiss, Y. Shiloh, Y. Ziv, Enhanced phosphorylation of p53 by ATM in response to DNA damage, Science 281 (1998) 1674–1677.
[16] X. Xu, L.M. Tsvetkov, D.F. Stern, Chk2 activation and phosphorylation-dependent oligomerization, Mol. Cell Biol. 22 (2002) 4419–4432.
[17] C.E. Canman, D.S. Lim, K.A. Cimprich, Y. Taya, K. Tamai, K. Sakaguchi, E. Appella, M.B. Kastan, J.D. Siliciano, Activation of the ATM kinase by ionizing radiation and phosphorylation of p53, Science 281 (1998) 1677–1679.
[18] E.P. Rogakou, C. Boon, C. Redon, W.M. Bonner, Megabase chromatin domains involved in DNA double-strand breaks in vivo, J. Cell Biol. 146 (1999) 905–916.
[19] Y. Andegeko, L. Moyal, L. Mittelman, I. Tsarfaty, Y. Shiloh, G. Rotman, Nuclear retention of ATM at sites of DNA double strand breaks, J. Biol. Chem. 276 (2001) 38224–38230.
[20] A.M. Taylor, D.G. Harnden, C.F. Arlett, S.A. Harcourt, A.R. Lehmann, S. Stevens, B.A. Bridges, Ataxia telangiectasia: a human mutation with abnormal radiation sensitivity, Nature 258 (1975) 427–429.
[21] C.J. Whitehouse, R.M. Taylor, A. Thistlethwaite, H. Zhang, F. Karimi-Busheri, D.D. Lasko, M. Weinfeld, K.W. Caldecott, XRCC1 stimulates human polynucleotide kinase activity at damaged DNA termini and accelerates DNA single-strand break repair, Cell 104 (2001) 1–11.
[22] Z. Li, T. Otevrel, Y. Gao, H.L. Cheng, B. Seed, T.D. Stamato, G.E. Taccioli, F.W. Alt, The XRCC4 gene encodes a novel protein involved in DNA double-strand break repair and V(D)J recombination, Cell 83 (1995) 1079–1089.
[23] S.E. Critchlow, R.P. Bowater, S.P. Jackson, Mammalian DNA double-strand break repair protein XRCC4 interacts with DNA ligase IV, Curr. Biol. 7 (1997) 588–598.
[24] U. Grawunder, M. Wilm, X. Wu, P. Kulesza, T.E. Wilson, M. Mann, M.R. Lieber, Activity of DNA ligase IV stimulated by complex formation with XRCC4 protein in mammalian cells, Nature 388 (1997) 492–495.
[25] J.I. Loizou, S.F. El Khamisy, A. Zlatanou, D.J. Moore, D.W. Chan, J. Qin, S. Sarno, F. Meggio, L.A. Pinna, K.W. Caldecott, The protein kinase CK2 facilitates repair of chromosomal DNA single-strand breaks, Cell 117 (2004) 17–28.
[26] K.H. Herzog, M.J. Chong, M. Kapsetaki, J.I. Morgan, P.J. McKinnon, Requirement for Atm in ionizing radiation-induced cell death in the developing central nervous system, Science 280 (1998) 1089–1091.
[27] Y. Lee, D.E. Barnes, T. Lindahl, P.J. McKinnon, Defective neurogenesis resulting from DNA ligase IV deficiency requires Atm, Genes Dev. 14 (2000) 2576–2580.
[28] N. Sugo, Y. Aratani, Y. Nagashima, Y. Kubota, H. Koyama, Neonatal lethality with abnormal neurogenesis in mice deficient in DNA polymerase beta, EMBO J. 19 (2000) 1397–1404.
[29] N. Gueven, O.J. Becherel, A. Kijas, P. Chen, O. Howe, J.H. Rudolph, R. Gatti, H. Date, O. Onodera, G. Taucher-Scholz, M.F. Lavin, Aprataxin a novel protein that protects against genotoxic stress, Hum. Mol. Genet. 13 (2004) 1081–1093.
[30] Y. Sano, H. Date, S. Igarashi, O. Onodera, M. Oyake, T. Takahashi, S. Hayashi, M. Morimatsu, H. Takahashi, T. Makifuchi, N. Fukuhara, S. Tsuji, Aprataxin, the causative protein for EAOH is a nuclear protein with a potential role as a DNA repair protein, Ann. Neurol. 55 (2004) 241–249.
[31] C. Chappell, L.A. Hanakahi, F. Karimi-Busheri, M. Weinfeld, S.C. West, Involvement of human polynucleotide kinase in double-strand break repair by non-homologous end joining, EMBO J. 21 (2002) 2827–2832.
[32] C. Brenner, Hint, Fhit, and GalT: function, structure, evolution, and mechanism of three branches of the histidine triad superfamily of nucleotide hydrolases and transferases, Biochemistry 41 (2002) 9003–9014.